Personal Climate Change

Roei Ben Zion, Dima Kisileiv, Daniella Glozman

Computer Science department, Tel Aviv University

GitHub

Figure 1: the 3 climate change effects we presented, the first (upper left) simulates flood in a street image, the second (upper right) simulates stormy weather in a sunny weathered image and the third (lower middle) simulates extreme heatwave.

Abstract

In this work, we aim to take advantage of the recent advancements in the fields of image generation and translation to build a tool that could help raise awareness to the climate change problem among the public, by simulating 3 selected effects of climate change on an input image. For each damage, we use a different method that in our view fits the best by both performance and resources needed to train it. For heatwaves, we use the classic CycleGAN [2] to learn a mapping to simulate the input image under the effect of an extreme heatwave. For floods, CycleGAN by itself yielded not sufficient results, so we adopt the InstaGAN [3] architecture and loss function, which is based on CycleGAN but specializes in translation of some instance in the image and preserving the rest of it. Finally, for stormy weather simulation, we use Neural Style Transfer [4]. This method is much less resource demanding and gives us an opportunity to experiment with another technology.

Introduction

Problem statement – In order to raise awareness to the climate change problem in public we adopt a somewhat straightforward approach, based on a cold assumption that people have a hard time relating to something that appears far from them. Hence, our goal is to show how some climate change effects would appear visually in an input environment image, hoping this personalisation would use as a good motivator to act.

Approach – We aimed to take advantage of the popular GAN [1] architecture and its variants because of its great performance in the image generation and translation fields and relatively well-established literature and information sources. We've chosen 3 damages of climate change – flooding, heatwaves and stormy weather, these choices are based on recent world events as well as the existence of accessible resources (e.g., data). Aiming for personalization, we focused on the Image-to-Image translation technologies, and more specifically unpaired Image-to-Image translation (I2I translation). In I2I translation we have 2 domains of images, A and B, and we are trying to find a meaningful mapping $G_A: A \rightarrow B$ while preserving the content

representations. In the paired I2I translation we are adding the assumption that every image $x \in A$ has a corresponding image $y \in B$ such that a meaningful translation exits between the 2. However, in most real-life applications, and especially in ours, it is not realistic to make this assumption, so we will work in an unpaired setting. For every effect, we will use domain A (source) as the domain of images without this effect and domain B (target) would be the images with this effect.

Methods

In the following we describe the methods we used for every damage separately, since we used different methods for each to get the best results given our resources. As there is a lack of clear consensus regarding reliable evaluation metrics for CycleGAN, we used user studies and empirical evaluation as evaluation metrics on the test set.

1. Heatwaves - Heatwaves have been a real-world problem in recent years, high temperatures are breaking records even in some areas where heat was not a serious problem before such as north America, Europe and more. We aim to show visually how an extreme heatwave could have looked like even in some areas that haven't experienced one yet. To achieve that, we set domain A to be images of locations with no visible heatwave, and domain B images of landscape of locations struck by a visible heatwave, we use the classic CycleGAN for the task. In the CycleGAN setting we train 2 generators and 2 discriminators G_A, G_B, D_A, D_B using some version of the GAN adversarial loss, and adding 2 constrains (for both sides) to get a meaningful mapping:

1 – the cyclic loss $L_{cyc} = ||G_B(G_A(x)) - x||_1$

2 – the identity loss $L_{idt} = ||G_B(y) - y||_1$

When $G_A: A \rightarrow B, G_B: B \rightarrow A, x \in A, y \in B$. We have adopted the Unet-based generator architecture introduced in the official implementation since it yielded much better results than the Resnet-based one. To choose the proper adversarial loss, we've experimented with 3 popular losses, the default least-squares loss, the hinge GAN loss, and the Wasserstein GAN (WGAN) loss [5]. We have also examined 3 regularization factors: Total Variation (TV) denoiser [6] perceptual and style as in [3] . We have found that the best combination is the WGAN loss when the discriminators parameters are clipped in $[-0.01, 0.1]$ and the TV denoiser, where we aim to minimize the difference between generated image pixels, hence our final loss function was:

$$L_{heat} = \lambda_1 L_{WGAN} + \lambda_2 L_{cyc} + \lambda_3 L_{idt} + \lambda_4 L_{TV}$$

When (assuming z is a generated image):

$$L_{WGAN} = E_{x \sim P_A}[D_A(x)] - E_{y \sim P_B}[D_A(G_B(y)] + E_{y \sim P_B}[D_B(y)] - E_{x \sim P_A}[D_B(G_A(x)]$$

$$L_{TV} = \sum_{i=1}^{H} \sum_{j=1}^{W-1} |z_{i,j} - z_{i,j+1}| + \sum_{i=1}^{H-1} \sum_{j=1}^{W} |z_{i,j} - z_{i+1,j}|$$

$$\lambda_1 = \lambda_2 = 10, \lambda_3 = 0.5, \lambda_4 = 10^{-5}$$

Figure 2: selected results of our model, the daylight images are the input.

We run the model with L_{heat} for 100 epochs on a dataset of around 200 images per domain that we've collected from the web.

2. Floods – out of the 3, floods simulation was the most complex task, and we've seen that CycleGAN (and some of its variants) fails to learn this translation. To solve this problem, we have decided to use a model named InstaGAN, which showed promising results in an instance aware translation, when the task is to translate some part of the image and preserve the rest. Differently from CycleGAN, the mapping InstaGAN aims to learn is from a paired domain of images and instances that are masked regions in each image to a similar structured domain, when the goal is to change only the generated masked part. In other words, we aim to learn $G_A: A \ X \ I_A \rightarrow B \ X \ I_B$ (where the instance in I_A is the road and sidewalk of every image) and the same for B (when the instance is the flooded part). To build such a dataset for the flooding task we need to be able to mask the flooded (water) part in domain B, and some part in the images of domain A we would want to see flooded (the road and sidewalk).

2.1 Segmentation – In order to be able to train an InstaGAN model, we had to create domains of images and corresponding masks. For the domain of images with floods (B), we masked the area where there's water, in domain A we've decided to segment roads, sidewalks etc. For domain A we used the famous CitySpaces [7] dataset that fortunately comes with a full semantic segmentation for every image. For the flood's domain, we have tried to build our own masking model to mask the water in an image, using Unet architecture and the Atlantis [12] dataset. We have compared this model to CSAIL segmentation model [8], and the latter showed better results, so we sticked with it for building our dataset's domain B.

2.2 Data preprocessing – The floods dataset, FloodIMG [9], contains many images that cannot be assumed to correspond meaningfully to CitySpaces. These images include rivers, aerial views, and other non-matching images. Furthermore, the dataset is quite large, comprising more than 5000 images, making it impractical to manually extract specific images.

We explored two different approaches to address this issue and trained the model using both methods. However, the results were similar for both approaches. In the first method, we utilized a ResNet backbone (by removing the last layer of ResNet18) that was pre-trained on ImageNet to extract semantic features from every flooded image and a sample of 150 randomly selected images from the CitySpaces dataset. We then averaged the feature maps of these 150 images. Subsequently, we measured the cosine similarity between each flooded image's feature map and the average feature map, selecting the top 1500 flood images.

The second approach involved creating a classifier to distinguish between street flood images (desired) and other images (such as rivers, aerial views, and less desirable images). This classifier was trained using 200 images in the training set (100 from each domain), all of which were manually collected and labeled from the FloodIMG dataset. We fine-tuned a pre-trained VGG16 network for this purpose. After running the classifier on the FloodIMG dataset, we obtained 1592 relevant images for domain B. The model presented in this work is the one trained on the dataset created by the classifier.

Figure 3: some examples of images from the FloodIMG dataset, when the lower images are not desired for translation because of their ariel view angle, and the above are desired.

2.3 Training – We train an InstaGAN model using a Resnet-based generator, and a least-squares adversarial loss for the GAN. Differently from the method used in the InstaGAN paper, we let the weight of the identity loss and the context loss to be 1/10 from the adversarial loss and the cycle loss in all our experiments as other configurations we tried yielded unstable results. Our final loss function in the baseline model is:

$$L_{floods} = \lambda_1 L_{LS-} + \lambda_2 L_{cyc} + \lambda_3 L_{idt} + \lambda_4 L_{ctx}$$

$$\lambda_1 = \lambda_2 = 10, L_{idt} = L_{ctx} = 1$$

Denoting $(x, a) \in A \ X \ I_A, (y, b) \in B \ X \ I_B, G_A(x, a) = (y', b')$ and $G_B(y, b) = (x', a')$:

$$L_{LS-GAN} = (D_A(x, a) - 1)^2 + D_A\big(G_B(y, b)\big)^2 + (D_B(y, b) - 1)^2 + D_B\big(G_A(x, a)\big)^2$$

$$L_{ctx} = \left\|w(a, b') \odot (x - y')\right\|_1 + \left\|w(b, a') \odot (y - x')\right\|_1$$

When $w(a, b')$ is the elementwise minimum (i.e., the intersected masked part) and $\odot$ is elementwise multiplication.

We trained InstaGAN for 300 epochs, using standard data augmentations (random cropping, flipping etc.).

Figure 4: some example results of the baseline floods model.

Although the baseline model has resulted in seemingly realistic results, we have examined different ways aiming to improve model performance. The image generation in the InstaGAN architecture consists of an encoder-decoder approach when the encoding phase occurs separately for the image and the segmentation, but the decoding phase involves the reconstruction of a concatenated image and segmentation, which makes it challenging to switch to a generator architecture without a clear separation between the encoder and decoder, such as the Unet-based approach used for the heatwaves part. Thus, we try some methods that could be applied 'on top' of the existing generator architecture.

We explored two different approaches. In the first, we investigated the impact of attention mechanisms that have shown promising results in image classification when integrated into Resnet blocks, such as CBAM (Convolutional Block Attention Module) [11] and SE (Squeeze and Excitation) [14]. In the second approach, we examined the effects of increasing the ratio between the parameter counts of the generators and discriminators. We'll call them the 'attention models' and the 'deeper model' respectively.

For the attention mechanisms, we show here that in contrast to the reported improvement of adding these mechanisms in the tasks of image classification or object detection, in our image translation task these mechanisms induce unstable results (when added the same way to Resnet blocks as [11], [14]).

Figure 5: a comparison of the CBAM model (left), SE model (middle) and the baseline model after 60 epochs of training.

We can see that at 60 epochs the baseline model is slightly better than the attention models. After 60 epochs we see no improvement in the attention models, but we see a significant improvement in the baseline model (as can be seen in the results). We've trained the attention models (CBAM, SE) for about 150 and stopped since we've seen no further change.

The motivation for the second approach was drawn from the heatwave model, where the discriminator had approximately 2.8 million parameters and the generator had roughly 11.4 million, resulting in a ratio just above 1:4. In contrast, our baseline flood model had a discriminator with around 9.8 million parameters and a generator with 26.7 million, resulting in a ratio of less than 1:3.

To address this, we introduced an additional convolution layer into the Resnet blocks within the generator. This block is iteratively used in the generation process. As a modification to the Resnet block configuration, we replaced the previous setup of 2 convolution layers followed by a residual connection with 3 convolution layers. This adjustment increased the parameter count to 37.4 million, bringing it closer to a 1:4 ratio.

As a result, these changes have led to more detailed results, as illustrated in the examples below.

Figure 6: a comparison between the deeper model (middle) and the baseline model (lower). In these examples, the areas indicated by the blue arrows demonstrate that the deeper model realistically portrays the shadows on the water, in contrast to the baseline model.

The deeper model accurately depicts the shadows on the water during a flood in a manner that corresponds to the presence or absence of objects on the surface, whereas the baseline model occasionally exaggerates the shadows on the water.

3. Stormy weather - In recent years, our world has witnessed a profound shift in weather patterns. While we've often associated extreme weather with certain regions, the lines between these climatic boundaries are blurring. Stormy weather, once a distant concern for some, is now impacting areas where it was historically rare. From winter thunderstorms in Israel to intense hurricanes in atypical locations, our planet's climate is undergoing a dramatic transformation. We aim to show visually how an extreme stormy weather could have looked like even in some areas that haven't experienced one yet. To achieve that, we set domain A to be images of sunny locations, and domain B images of storms, rains, clouds and etc. We've used the style transfer method for the task. We've used the default least-squares loss and a pretrained VGG-19 model. We have also examined 2 regularization factors: Total Variation (TV) denoiser [6], and sharpness loss [13] defined as the mean of L_1 norm differences between x the input and:

$$blurred = avgpool(x)$$

Style loss uses gram matrix calculation within the loss. We added calculations for style and content losses in the convolutional layers and to make the results more real and less art-wise, we added content layers in conv layers that capture features relevant to realism.

VGG-19 model uses ReLu as an activation function, and contains max pooling layers, conv layers, batch normalization layers and fully connected layers. We added image normalization as a first layer with ImageNet mean and standard deviation which is the convention for image normalization in pre-trained models.

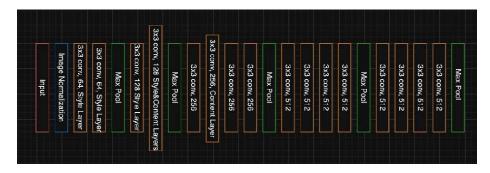We ran the model for 500 epochs.

Figure 7: model architecture.

We have found that the best combination is the following:

$$L_{storms} = \lambda_1 L_{style} + \lambda_2 L_{content} + \lambda_3 L_{sharpness}$$

When we set:

$$\lambda_1 = 1.8 * 10^5, \lambda_2 = 1, \lambda_3 = 0.1$$

Future work

In this work, we propose various methods and training approaches to harness unpaired image-to-image translation technologies for raising awareness about climate change. While we have demonstrated the potential with the examples mentioned, it's important to note that addressing other climate change effects, such as air pollution or forest fires, is a possibility. However, each effect necessitates careful data collection and preprocessing, as prepared datasets are often rare. Selecting the right model for achieving realistic results and the extensive training process are also vital considerations.

In the case of CycleGAN-based methods, achieving 'perfect personalization,' where the damage can be integrated into any input scene, requires the creation of a highly diverse and substantial dataset to encompass various types of input images. Our models excel when applied to images with a structure similar to those in their training datasets (e.g., our flood model works well with images resembling those in the CitySpaces dataset). However, they may encounter challenges when handling images that significantly deviate from the dataset distributions.

References

[1] J. P.-A. M. M. B. X. D. W.-F. S. O. A. C. Y. B. Ian J. Goodfellow, "Generative Adversarial Networks".

[2] T. P. P. I. A. A. E. Jun-Yan Zhu, "Unpaired Image-to-Image Translation using Cycle-Consistent Adversarial Networks".

[3] M. C. J. S. Sangwoo Mo, "InstaGAN: Instance-aware Image-to-Image Translation".

[4] A. S. E. M. B. Leon A. Gatys, "A Neural Algorithm of Artistic Style".

[5] S. C. L. B. Martin Arjovsky, "Wasserstein Generative Adversarial Networks".

[6] C. R. V. a. M. E. Oman:, "Iterative Methods for Total Variation Denoising".

[7] M. O. S. R. T. R. M. E. R. B. U. F. S. R. B. S. Marius Cordts, "The Cityscapes Dataset for Semantic Urban Scene Understanding".

[8] B. a. Z. H. a. P. X. a. X. T. a. F. S. a. B. A. a. T. A. Zhou, "Semantic understanding of scenes through the ade20k dataset," *International Journal on Computer Vision.*

[9] R. K. a. R. P. a. V. Samadi, "FloodIMG: Flood Image DataBase System," *Kaggle.*

[10] I. G. W. Z. V. C. A. R. X. C. Tim Salimans, "Improved Techniques for Training GANs".

[11] J. P. J.-Y. L. I. S. K. Sanghyun Woo, "CBAM: Convolutional Block Attention Module".

[12] S. M. H. a. W. Z. a. W. X. a. W. S. a. G. E. Erfani, "ATLANTIS: A benchmark for semantic segmentation of waterbody images".

[13] A. K. H. M. B. N. Pierre Foret, "Sharpness-Aware Minimization for Efficiently Improving Generalization".

[14] L. S. S. A. G. S. E. W. Jie Hu, "Squeeze-and-Excitation Networks".

[15] R. G. P. D. Z. T. K. H. Saining Xie, "Aggregated Residual Transformations for Deep Neural Networks".